Accurate Multi-resolution Discrete Search Method to Estimate the Number and Directions of Axon Packs from DWMRI

Ricardo Coronado-Leija[1], Alonso Ramirez-Manzanares[1], Jose Luis Marroquin[1], and Rolando Jose Biscay[1]
[1]*Computer Science Department, Centro de Investigacion en Matematicas, Guanajuato, Guanajuato, Mexico*

Purpose: The accurate voxel-wise estimation of white matter tissue properties from Diffusion Weighted MR benefits the building of connectivity brain maps and disease detection. Unlike models based on the computation of orientation distribution function[1] (ODF) and fiber orientation distribution[2] (FOD), the multi-compartment models[3] provide most of the tissue parameters directly, avoiding optimization and prone-to-error threshold-based post-processing steps to locate the principal diffusion directions (PDD). In the parametric multi-compartment Gaussian Mixture Model (GMM) each PDD is characterized by the spectral decomposition of the diffusion tensors D_k, where the normalized MR diffusion signal $A_i = (S_i/S_0)$ at voxel r is modelled as $A_i(r) = \sum_{k=1}^{N} \alpha_k \exp(-b g_i^T D_k(r) g_i), i = 1,2,\dots,M$, N is the number of axon bundle packs, M is the number of diffusion encoding orientations (DEO) g_i, and α_k denotes the volume fraction of each D_k. Direct least squares (LS) fitting of the GMM presents two drawbacks: N has to be provided *a priori*, and it is a hard-to-solve starting-point-dependent non-linear optimization procedure. We present here a stable, accurate and robust-to-noise method to fit the GMM for a long range of crossing angles. The method improves the well-known Constrained Spherical Deconvolution method[2] (CSD) both in angular resolution and in the estimation of the number of axon bundles at challenging configurations, namely, small crossing angles (< 45º) [4]. Such detailed information helps to identify fanning structures in the brain that can be properly exploited by recent tractography methods[5].

Methods: The proposed Multi-resolution Discrete Search (MRDS) method is based on three key ideas: 1) A MRSD to determine the PDD's; 2) The parameter-free determination of the number of axon bundles using the Bayesian Information Criterion (BIC) and 3) A Simultaneous Denoising and Fitting (SDF) procedure to achieve robustness with respect to noise. We impose radial symmetry $\lambda_1 \gg \lambda_2 = \lambda_3$ on the $D_k = R(\theta_k,\varphi_k) diag(\lambda_1,\lambda_2,\lambda_3) R^T(\theta_k,\varphi_k)$ with rotation matrices $R(\theta_k,\varphi_k)$ associated to orientations (θ_k,φ_k). By fixing λ_1, λ_2, N and $(\theta_k,\varphi_k), k = 1,2,\dots,N$, the GMM is simplified to $A_i = \sum_{k=1}^{N} \alpha_k \Phi_i(\theta_k,\varphi_k) = \sum_{k=1}^{N} \alpha_k \Phi_k^i$, where the column $\Phi_k \in \mathbb{R}^M$ is a dictionary atom[6]. The remaining unknowns α_k are computed by minimizing the LS error $\epsilon = \sum_{i=1}^{M} \left(A_i - \sum_{k=1}^{N} \alpha_k \Phi_k^i\right)^2$ where the LS $N \times N$ linear system s.t. $0 \le \alpha_k \le 1$, is solved by the projected Gauss-Seidel algorithm. Given a low-resolution orientation set $\mathcal{L}$ with cardinality $|\mathcal{L}|$ (Fig 1a), the first MRDS stage computes the dictionary $\Phi \in \mathbb{R}^{M \times |\mathcal{L}|}$ with $\lambda's$ as in [2,6]. For each combination $\binom{|\mathcal{L}|}{N}$, it minimizes ϵ for α and keeps the combination of atoms with minimal ϵ. Using this preliminary solution of N orientations, the second MRDS stage refines the solution by using a high-resolution orientation set $\mathcal{H}$ with cardinality $|\mathcal{H}| \gg |\mathcal{L}|$ (Fig. 1b). The method selects the orientations from $\mathcal{H}$ that are in the neighboring cone of the optimal N orientations from $\mathcal{L}$ (Fig. 1c). The same GMM fitting strategy (in stage one) is repeated for the signal atoms associated to the selected orientations from $\mathcal{H}$ (Fig. 1d). The method applies the algorithm for $N = 1, 2\ y\ 3$. The model selection problem is then solved by keeping the N that minimizes $BIC^7 = 2\epsilon/\sigma^2 + p\ln(M)$, where $p = 5N$ is the degrees-of-freedom for each model, and σ^2 is the noise's variance. An SDF strategy, similar to the *simultaneous sparse coding*[8], is applied to reduce the effect of the noise in the MR signal. For each voxel r, let $\mathcal{N}_r$ be the set of voxels in its $3D$ $5 \times 5 \times 5$ spatial neighborhood, such that the MSE between their A signals and those of the reference voxel r is smaller than $2\sigma^2$. The voxels in $\mathcal{N}_r$ are jointly used to fit the GMM (with the MRDS), and the same set of atoms is assigned to all voxels in $\mathcal{N}_r$, (although the α_k's are computed independently for each voxel). After this process is completed, each voxel r will have several models (sets of atoms) assigned to it (one for each neighborhood it belongs to), so for each r, voting and averaging procedures are used to compute the number of atoms and the model parameters, resp.

Results: The $32 \times 32 \times 1$ synthetic dataset schematized in Fig. 2 comprises two fiber bundles with crossing angles between $0°$ and $90°$, equal volume fractions, and $FA = 0.77$ in the underlying Gaussian model for the individual tracts. 66 single-shell DEO with b= $3000\ s/mm^2$ are used. The simulated signals were corrupted by Rician noise with SNR on S_0 equal to 20. We compare with the CSD algorithm[2] (code provided by the author): $l_{max} = 10$; threshold for false positive peaks on the FOD equal to 0.2 of the maximum value[9]. We compute the *success rate (SR:* fraction of voxels with the correct number of fiber populations), and the *Average Angular Error (AAE)* w.r.t. the ground truth. Figs. 3a and 3b show the results for the configuration depicted in Fig. 2. We note that MRDS and MRDS-SDF present a higher SR at large (>40º) and small (25° to 40°) separation angles, while CSD systematically reports one fiber bundle on angles <40°. For the AAE, the CSD and the MRDS have similar results (below 5°) for crossing angles greater than 55°. In the interval $40° - 55°$ we observe a big increase of the AAE for the CSD (up to 16°) while the MRDS keeps it smaller than 6°. By using MRDS-SDF the AAE decreases achieving errors below 3° for crossing angles greater than 30°. Maps of estimated N for CSD and MRDS-SDF on data field of Fig. 2 are shown in Fig 5. We explore the sensitivity of the methods to different λ values on $SNR = 20$ data, since the user must provide them in the initial estimation step (actual λ's are $[1 \times 10^{-3}, 0.2 \times 10^{-3}]$). Fig. 4 shows results for 50° crossing angle, λ_1 and λ_2 vary in the ranges $[0.5,1.5] \times 10^{-3}$ and $[0.0,0.3] \times 10^{-3}$. SR and AAE are plotted on first and second rows, respectively. Columns of Figs. 4a/4d, 4b/4e and 4c/4f show the sensitivity of CSD, MRDS, and MRDS-SDF. We observe that both versions of our proposal report a SR of 100% and a better AAE on a broader region than CSD. The results of MRDS above remain consistent with an exhaustive validation with 1000 trials per crossing angle in the range [0º, 90º] (not shown). Fig. 6 and 7 present the ODFs of MRDS-SDF on the *in vivo* multi-shell (b_1=700,b_2=3000) human brain data provided with the NODDI toolbox (mig.cs.ucl.ac.uk/index.php?n=Tutorial.NODDImatlab); the PDDS are spatially coherent and capture the expected complexity at the crossing of *corpus callosum*, *corticospinal tract* and *superior longitudinal fasciculus* (ROIs on Fig. 8).

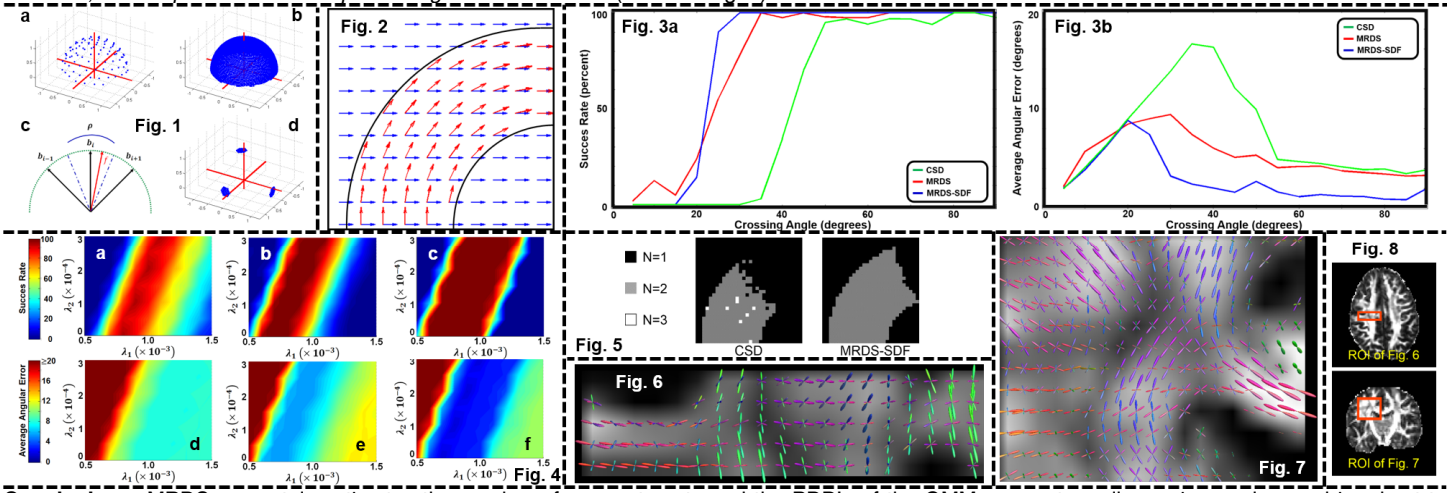

Conclusions: MRDS accurately estimates the number of compartments and the PDD's of the GMM, even at small crossing angles, and is robust to variations on the chosen λ values. On all experiments, our proposal presents better performance than CSD, with MRDS-SDF presenting the best results.

References: [1] D.S. Tuch, Magn Reson Med, 2004. [2] J.D. Tournier et al Neuroimage, 2007. [3] D.S. Tuch et al, Magn Reson Med, 2002. [4] A. Daducci et al, Trans Med Imag, 2014. [5] M. Rowe et al, Inf. Proc. in Med Imag, 2013. [6] A. Ramirez-Manzanares et al, Trans Med Imag, 2007. [7] Panagiotaki et al NeuroImage, 2012. [8] J. Mairal et al 12th Int. Conf. on Comp. Vis., 2009. [9] Jeurissen et al. Hum Brain Mapp, 2013.